

## Supplementary Figure Legends

**Supplementary Figure 1.** Generation of *Nyap1*, 2, and 3 knockout mice. (A-C) Schematic representation of the wild-type (WT) allele and the targeting vectors for *Nyap1* (A), *Nyap2* (B), and *Myo16/Nyap3* (C). Exons are indicated by filled boxes. NEO, neomycin-resistance gene; TK, thymidine kinase gene.

**Supplementary Figure 2.** High expression of NYAPs mRNA in the cortex around perinatal days. (A-H) Brain cryosections obtained from WT mice of the indicated ages were hybridized with *Nyap1*, 2, or 3 mRNA probes. WT sections were mounted on the same glass slides containing sections from corresponding *Nyap1*, 2, or 3 KO mice as negative controls (see Figure 2C and D). Coronal sections of the motor cortex at the level of posterior striatum are presented. Cortical regions are indicated on the right (cp).

**Supplementary Figure 3.** Interactions between the NYAPs and PI3K p85 $\beta$  in HEK293T cells. The membranes used in Figure 6D-F were reprobbed with an anti-PI3K p85 $\beta$  antibody. Briefly, HEK293T cells were transfected with GST, GST-NYAP1(1-832), GST-NYAP2(1-748), or GST-NYAP3(1109-1919). The cell lysates were pulled down with glutathione sepharose (GE healthcare) and immunoblotted with an anti-PI3K p85 $\beta$  antibody, and interaction between GST-NYAPs and endogenously-expressed PI3K p85 $\beta$  were tested.

**Supplementary Figure 4.** Membrane localization of the NYAPs. The membrane fraction isolated

from P1 mouse brains was probed with the 4G10 anti-phosphotyrosine antibody to detect the NYAPs.

**Supplementary Figure 5.** Expression levels of Akt, ERK1/2, and  $\alpha$ -tubulin in WT and TKO P1 mouse brains. WT and TKO brains were lysed in TNE buffer, and protein concentration was measured with the BCA protein assay kit (Pierce). Twenty microgram of the lysates were separated by SDS-PAGE and probed with the indicated antibodies. Protein levels of Akt, ERK1/2, and  $\alpha$ -tubulin were quantified (WT, n = 4; TKO, n = 4). n.s.: not significant.

**Supplementary Figure 6.** BDNF-induced Akt activation in WT and TKO neurons. Cultured cortical neurons obtained from WT and TKO brains were stimulated with 200 ng/ml BDNF for the indicated time periods at DIV 2. Activity of Akt and ERK1/2 were measured as in Figure 5.

**Supplementary Figure 7.** Interactions between the NYAPs and Nap1, Sra1, GRAF, and ACOT9 in HEK293T cells. (A-D) Interactions between the NYAPs and Nap1 (A), Sra1 (B), GRAF (C), and ACOT9 (D). HEK293T cells were transfected with the indicated plasmids. The NYAPs were immunoprecipitated with anti-EGFP (A and C) or anti-FLAG (B and D) antibodies, and immunoblotted with anti-FLAG (A and C), anti-Myc (B), and anti-EGFP (D) antibodies.

**Supplementary Figure 8.** Interactions between NYAP2 and WAVE1 in HEK293T cells. HEK293T cells were transfected with FLAG-WAVE1 and GST or various deletion mutants of

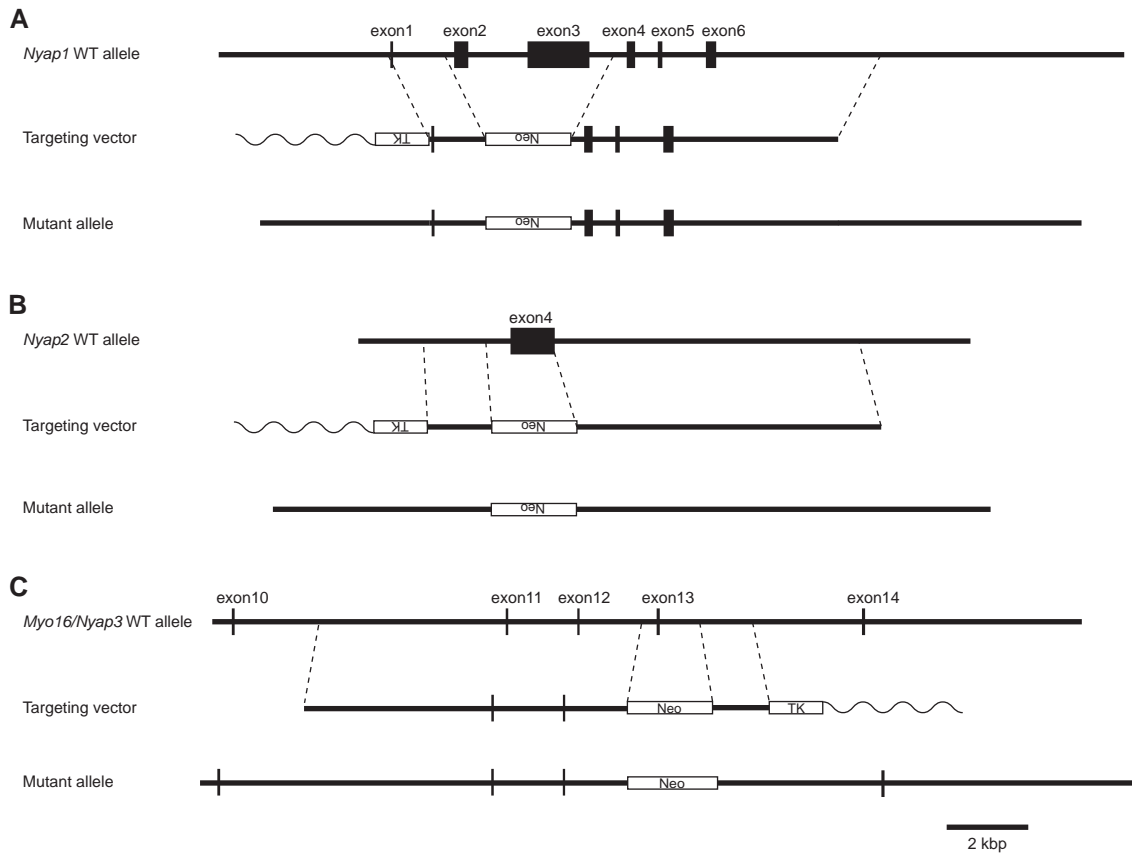
GST-tagged NYAP2 as indicated. The cell lysates were incubated with glutathione sepharose (GE healthcare) and immunoblotted with an anti-WAVE1 antibody.

**Supplementary Figure 9.** Interactions between the NYAPs and WAVE1 in the mouse brain. The lysates obtained from WT and TKO P1 mouse brains were immunoprecipitated with an anti-WAVE1 antibody. The immunoprecipitates were probed with the 4G10 anti-phosphotyrosine antibody to detect phosphorylated NYAPs.

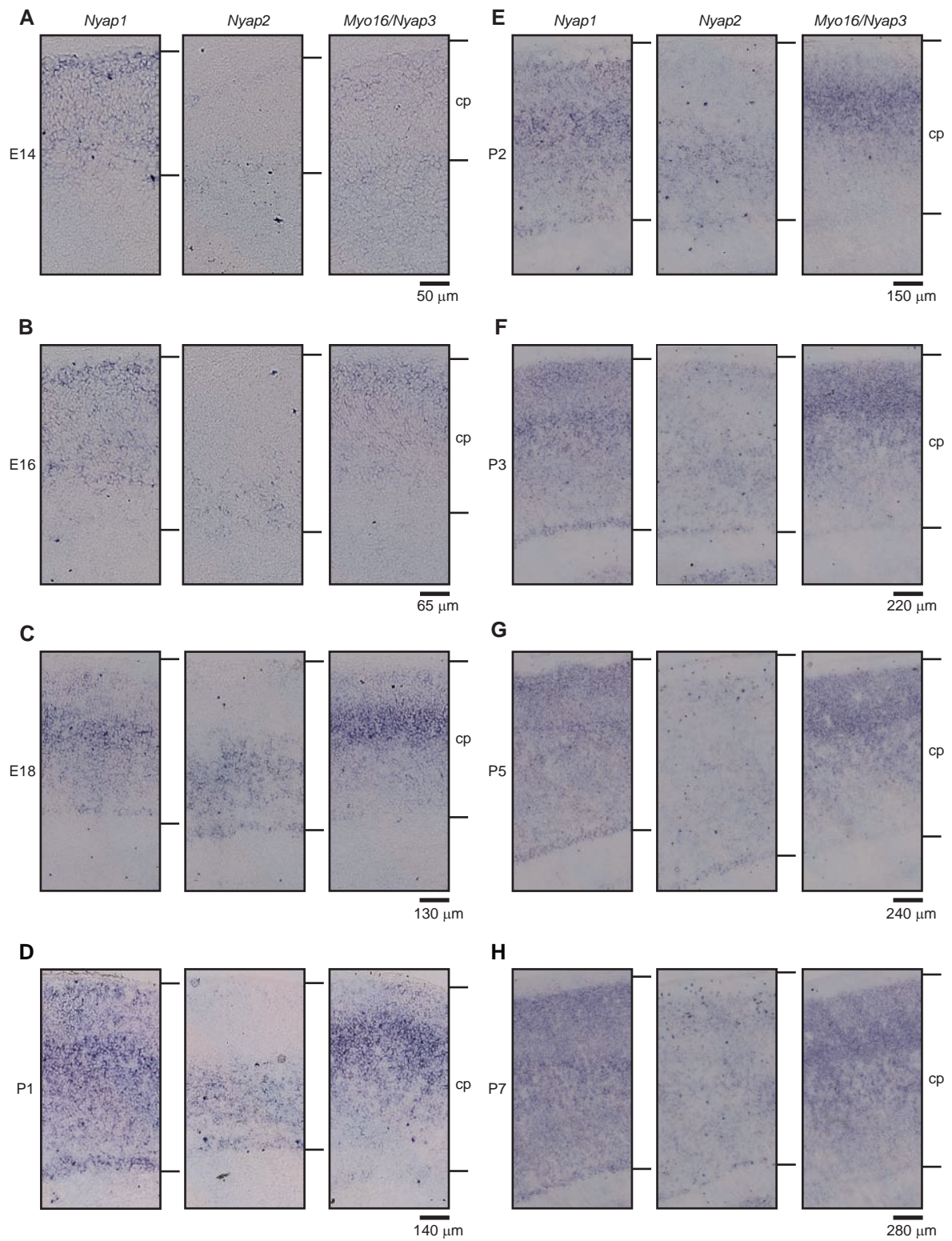
**Supplementary Figure 10.** NYAPs-mediated remodeling of the actin cytoskeleton. **(A-R)** Requirement of PI3K- and WAVE1-interacting regions in the NYAPs for remodeling of the actin cytoskeleton in HeLa cells. HeLa cells were transfected with various mutants of GST-tagged NYAPs as indicated, and stained as in Figure 8. Actin stress fibers are indicated by white arrowheads. Cytosolic accumulation of collapsed actin fibers is indicated by black arrowheads. Scale bar: 50  $\mu\text{m}$ .

**Supplementary Figure 11.** Developmental changes in the expression levels of NYAPs-interacting proteins in the brain. Total brain lysates obtained from mice of the indicated ages were immunoblotted with indicated antibodies. NYAP2 protein expression was detected with the N24 rabbit anti-NYAP2 antibody after immunoprecipitation with the N2M1 mouse anti-NYAP2 antibody to improve sensitivity and specificity. Brain lysates of TKO P1 mice were included as negative controls to ensure the specificity of anti-NYAP1, 2, and 3 antibodies. The effector WAVE1 core complex (composed of Nap1, Sra1, and WAVE1) was expressed constantly, but proteins with

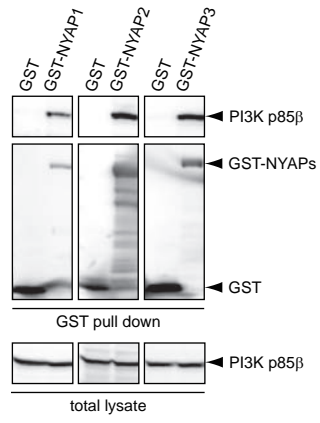
regulatory roles (Contactin5, Fyn, NYAPs, and PI3K) were highly expressed around perinatal days (see Figure 4F for PI3K expression).



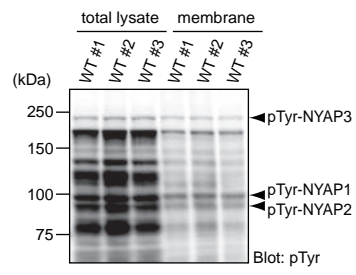
**Supplementary Figure 1.** Generation of *Nyap1*, *2*, and *3* knockout mice.



**Supplementary Figure 2.** High expression of NYAPs mRNA in the cortex around perinatal days.

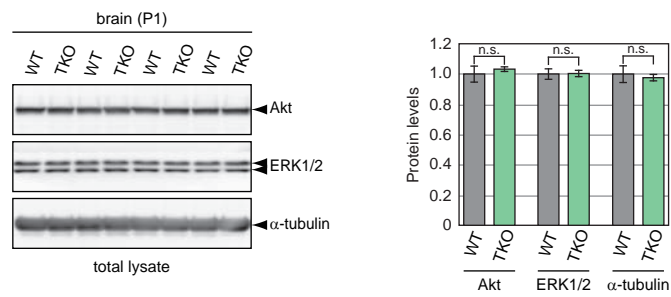


**Supplementary Figure 3.** Interactions between the NYAPs and PI3K p85 $\beta$  in HEK293T cells.

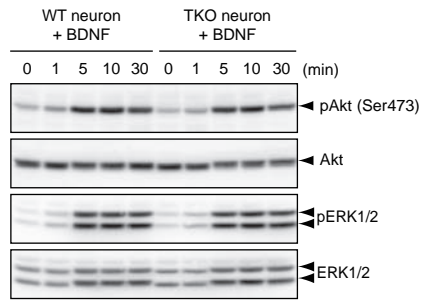


**Supplementary Figure 4.** Membrane localization of the NYAPs.

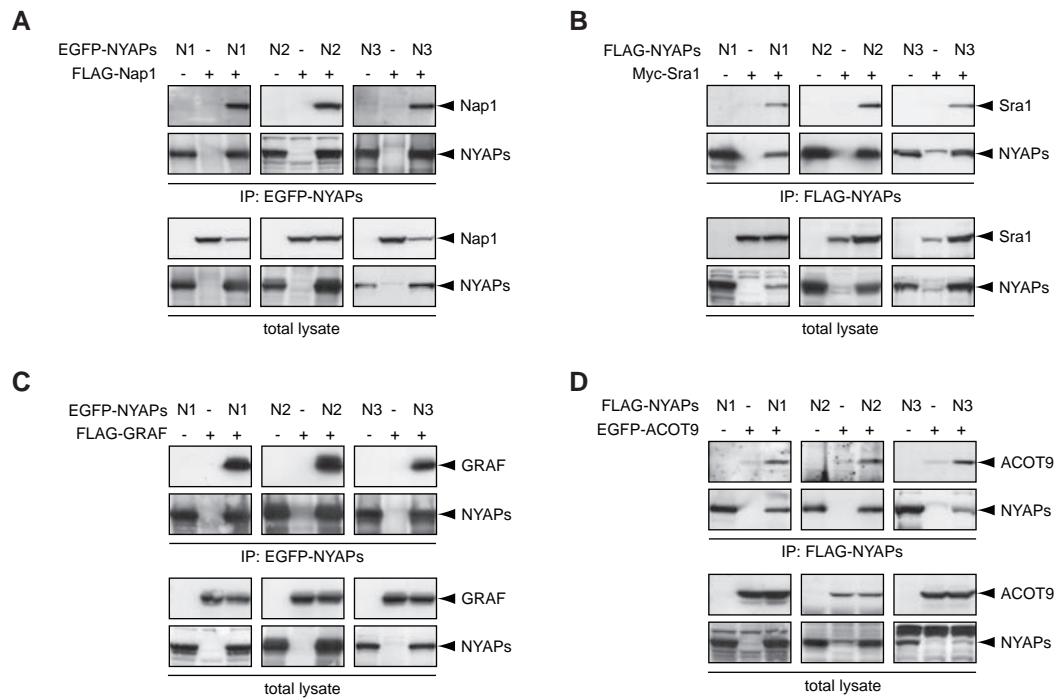




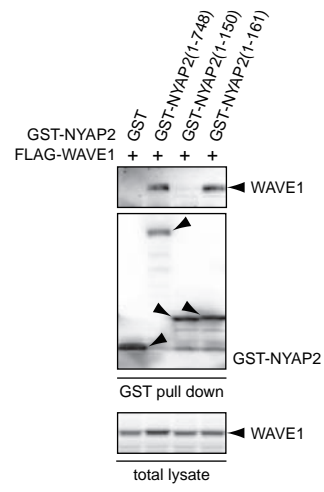
**Supplementary Figure 5.** Expression levels of Akt, ERK1/2, and  $\alpha$ -tubulin in WT and TKO P1 mouse brains.



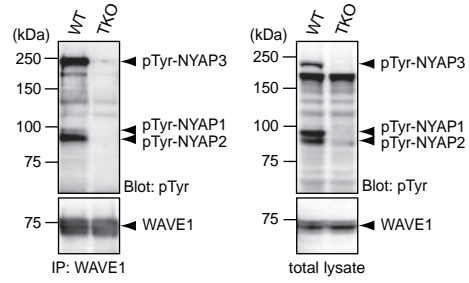
**Supplementary Figure 6.** BDNF-induced Akt activation in WT and TKO neurons.



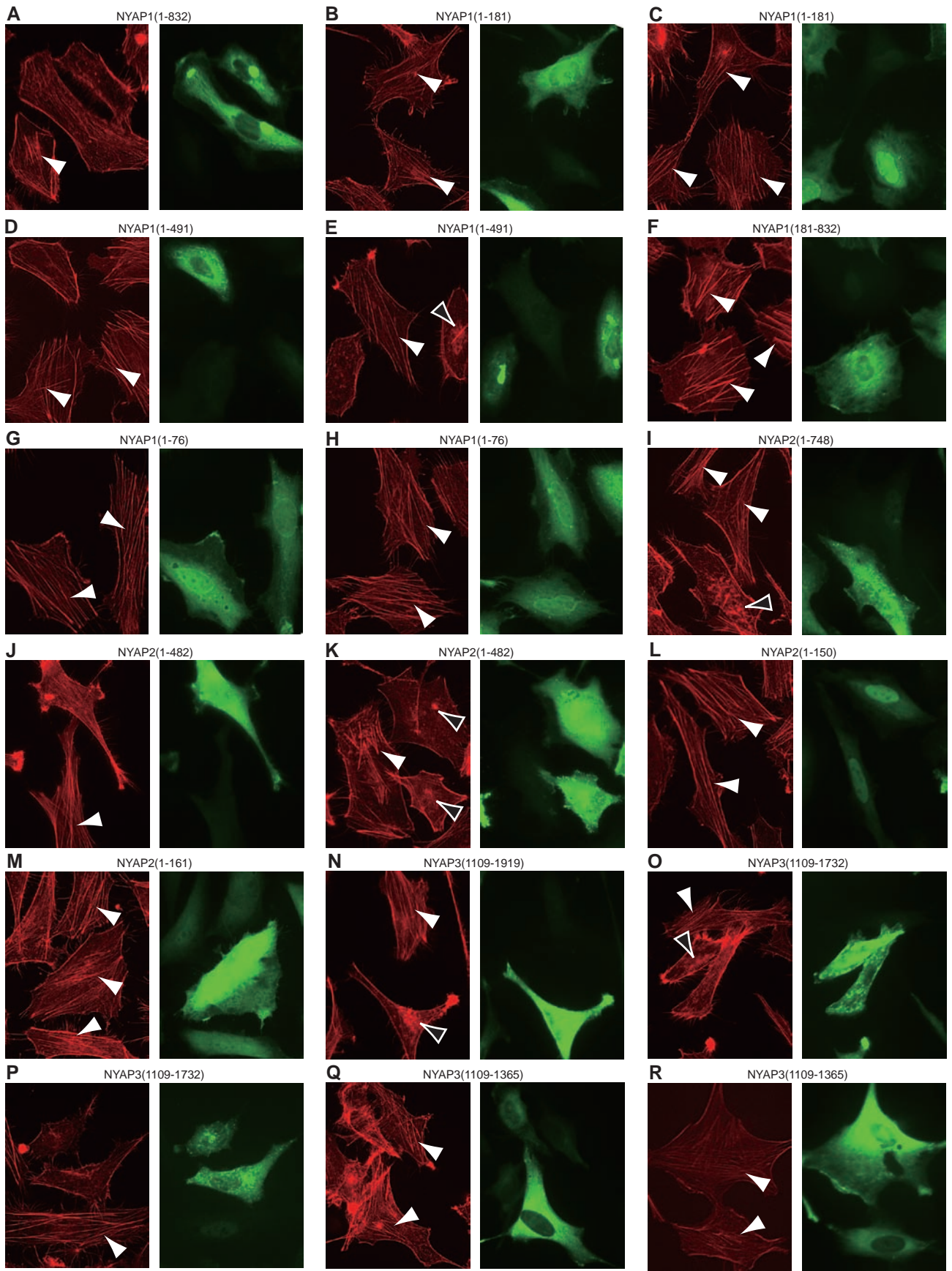
**Supplementary Figure 7.** Interactions between the NYAPs and Nap1, Sra1, GRAF, and ACOT9 in HEK293T cells.



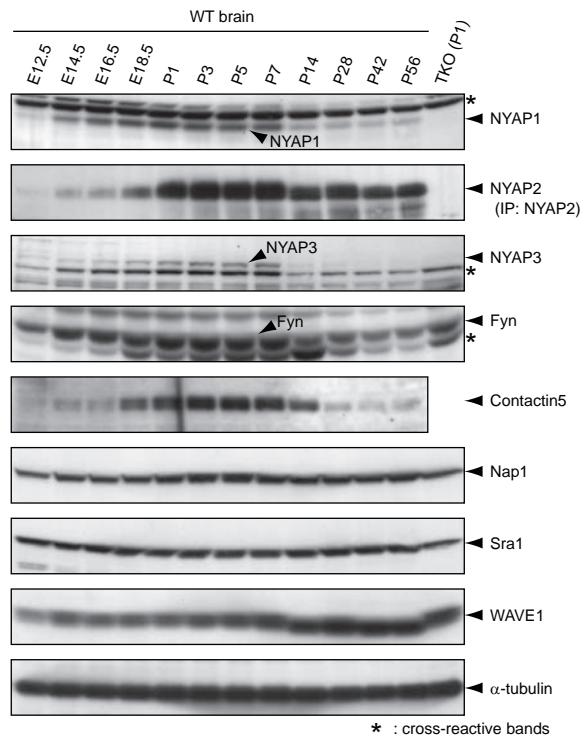
**Supplementary Figure 8.** Interactions between NYAP2 and WAVE1 in HEK293T cells.



**Supplementary Figure 9.** Interactions between the NYAPs and WAVE1 in the mouse brain.



Supplementary Figure 10. NYAPs-mediated remodeling of the actin cytoskeleton.



**Supplementary Figure 11.** Developmental changes in the expression levels of NYAPs-interacting proteins in the brain.